Mechanochromism and Polymorphism-Dependent Emission of Tetrakis(4-(dimethylamino)phenyl)ethylene

6 AUTHORS, INCLUDING:

Bin Xu
Jilin University
95 PUBLICATIONS   **1,888** CITATIONS

SEE PROFILE

Bao Li
Jilin University
65 PUBLICATIONS   **1,003** CITATIONS

SEE PROFILE

Sean Xiao-An Zhang
Jilin University
49 PUBLICATIONS   **511** CITATIONS

SEE PROFILE

Mechanochromism and Polymorphism-Dependent Emission of Tetrakis(4-(dimethylamino)phenyl)ethylene

Qingkai Qi, Jibo Zhang, Bin Xu,* Bao Li, Sean Xiao-An Zhang, and Wenjing Tian*

State Key Laboratory of Supramolecular Structure and Materials, Jilin University, Changchun 130012, Jilin, P. R. China

Ⓢ Supporting Information

ABSTRACT: The mechanochromic property of tetrakis(4-(dimethylamino)phenyl)ethylene (TDMAPE) with natural propeller shape and nearly centrosymmetric structure was investigated. The destruction of the crystalline structure leads to the planarization of molecular conformation, which is considered as a possible reason for the red-shift of absorption and fluorescence spectra after grinding. And the polymorphism-dependent emissions of the two polymorphs of TDMAPE are mainly determined by the intramolecular conformation, which show the increased coplanarity or conjugation degree, ultimately leading to the bathochromic shift of the emissions.
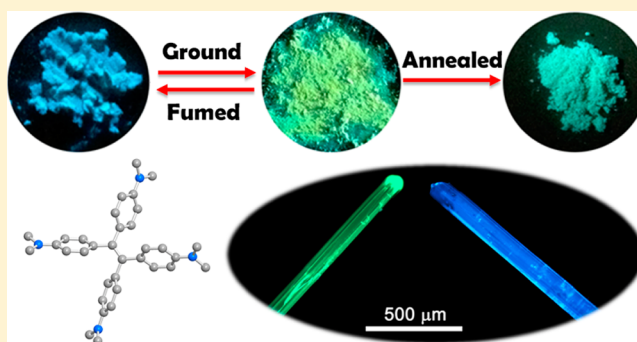
■ INTRODUCTION

Mechanochromic (piezochromic) materials can change their emission colors in response to appropriate external force stimulus such as shearing, grinding, or pressing.[1] As a kind of "smart material", mechanochromic materials have attracted significant attention because of their promising applications in optical storage, pressure sensors, rewritable media, and security ink.[2−12] Different from solid-state chemical reaction, controlling the mode of molecular packing (aggregation states) or intramolecular conformation to realize mechanochromism is more attractive for both fundamental research and practical applications due to low pressure demand and good reversibility.[13]

It has been revealed that the mechanochromic performances are usually related to the phase transition between the crystalline state and amorphous phase.[14] Because of the pressurized sample possesses amorphous nature, its molecular packing modes and configuration could not be readily verified, which increases the difficulty in determining the inherent reasons for emission shift. So far, changes in intramolecular planarity,[15−17] as well as intermolecular interactions of $\pi-\pi$ stacking,[18−20] and H- or J-aggregation[21] have all been assigned as the causes of the mechanochromic phenomenon.

Tetraphenylethylene (TPE), as a prototype aggregation-induced enhanced emission (AIEE) molecule, has no luminescence in solution but exhibits strong luminescence in the aggregation state. Because of its facile synthesis and outstanding AIEE effect, molecules based on TPE have been widely used in the field such as chemical sensors, organic light-emitting devices, biological labels, etc.[22−29] Because of the natural propeller shape of TPE, intermolecular $\pi-\pi$ stacking can be prevented in the solid state. Moreover, the centrosymmetric structure also makes H- or J-aggregation

unlikely happen in the aggregation state of TPE-based molecules. These features make TPE-based molecule an ideal model to investigate the conformational effects on molecular emissions. Thus, molecules based on TPE bearing the mechanochromic property have received a widely concern.[30,31] Recently, Tang et al. have reported some alkoxy-substituted tetraphenylethylene (TPE) derivatives and demonstrated their morphology-dependent multicolor emissions by different external stimuli in solid state.[32,33] The twisted conformation of these molecules rule out any specific strong intermolecular interactions (such as $\pi-\pi$ stacking or H/J-aggregates) in its aggregates due to the steric hindrance. So the author infers the difference of the emission color may be ascribed to the conformation of the independent molecule in different aggregates. As usual, different polymorphs of organic molecules exhibit different luminescence properties, which can provide a way to study the effect of intramolecular conformation, packing patterns, and intermolecular interactions on luminescence properties directly. Nevertheless, only few reports could get obviously different emission crystals and further to infer what happens to the molecules after grinding or under pressure. Tang and Zhang both have reported polymorphism-dependent emission of di(p-alkoxylphenyl)dibenzofulvene and revealed their reversible switching of the emission by thermal and mechanical stimuli.[34,35] Park has shown polymorphic and mechanochromic luminescence modulation in the highly emissive dicyanodistyrylbenzene crystal.[36] Fraser has discovered polymorphism and reversible mechanochromic luminescence for solid-state difluoroboron avobenzone.[37] Our group have

previously reported two polymorphs of tetrakis(4-methoxyphenyl)ethylene and demonstrated the effect of single molecular conformation on fluorescence.[38]

In this article, we investigate the mechanochromism and polymorphism-dependent emission of one of the TPE derivatives TDMAPE. The covalent linking dimethylamino groups into TPE brings the intermolecular interactions (such as C−H···π and C−H···N interactions), and these relative "soft interactions" will be easily broken after grinding or under pressure. Then the resulting change of packing patterns or intramolecular conformation will finally make mechanochromism possible to realize. Furthermore, the obtained two polymorphs of the compound with totally different emission and packing pattern provide a good opportunity for us to investigate conformational effects on molecular emissions. The comparison of the two single crystals indicates that the better intramolecular coplanarity or conjugation degree is the main cause for the red-shift of the emission under pressure.

■ RESULTS AND DISCUSSION

TDMAPE was prepared conveniently by typical McMurry reaction[39] according to the synthetic routes shown in Scheme 1. Detailed characterizations of the product are described in the Supporting Information.

Scheme 1. Synthetic Route to TDMAPE
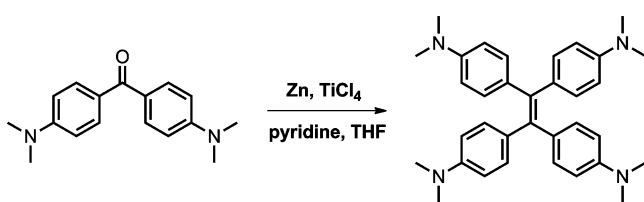
To investigate the AIEE characteristic of TDMAPE, its fluorescent behavior was studied. Figure 1 shows the PL change and fluorescent images of TDMAPE in THF and THF/water mixtures. When the water fraction (f_w) is lower than 80%, the PL curve is almost flat lines parallel to the abscissa, which means the compound is nearly nonemissive in THF, a good solvent for TPE. This can be ascribed to the free rotation of carbon−carbon single bonds between the four periphery phenyls and the ethylene core which dissipates the whole excited luminogens and finally results in fluorescence quenching in dilute solutions.[40−43] However, the emission turns on when large amounts (>80%) of water, a poor solvent for TPE, were added into the THF solution of the sample. When the water fraction reaches to 90%, its PL intensity is 64-fold higher than that in pure THF. The increased fluorescent intensity can be attributed to the formation of molecular aggregates, in which the restricted intramolecular rotations led to increased fluorescence emission.[44−49] Meanwhile, the emission peak of the aggregates red-shifts 60 nm from 460 to 520 nm when the water fraction increases from 80% to 90%. After investigation of the morphology of the aggregates by transmission electron microscope (TEM) and electron diffraction (ED) (Figure S1), it indicates that the aggregates formed in 80% (f_w) mixture are crystalline state while in 90% (f_w) mixture are amorphous state.

The mechanochromic performance of TDMAPE has been studied by both absorption and fluorescence spectra. The pristine powder of TDMAPE with blue emission was obtained
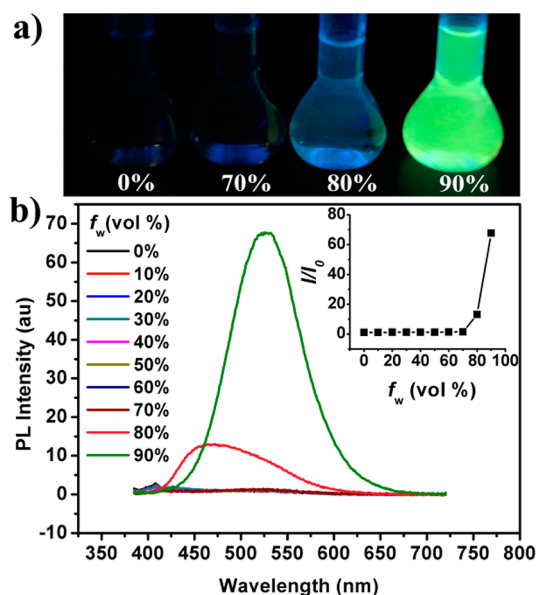
Figure 1. (a) Fluorescent images of the compound in different water fraction mixtures under 365 nm UV illumination. (b) Fluorescence spectra of TDMAPE (1×10^{-5} M) in THF and water mixtures with different water fractions (f_w). Inset: plot of I/I_0 versus water fraction, where I and I_0 represent the fluorescence intensities in a THF/water mixture with a specific f_w and in pure THF, respectively.

from column chromatography with a mixture eluent (ethyl acetate and petroleum ether) and show excellent mechanochromic performances. Appreciable change in both visible color and UV/vis absorption band was observed before and after grinding the powder (Figure 2a,d). The maximal absorption band of ground sample shows an obvious red-shift. At the same time, the fluorescence of the pristine sample can also change from blue (Em: 470 nm) to yellow-green (Em: 528 nm) by grinding (Figure 2b,c). The red-shift of the absorption and fluorescence spectra after grinding may originate from the increased conjugation with decreased the optical bandgap of the molecules in the ground sample. Then the maximal absorption band and the fluorescence peak can almost turn back upon fumed by ethyl acetate (EtOAc). But after annealing the ground sample at 150 °C for 1 min, its emission turns from yellow-green (Em: 528 nm) to green (Em: 492 nm), which is different from that fumed by solvent. It seems that the sample formed after grinding did not re-form to the pristine blue emission sample upon heating but transformed to green emission sample. The mechanochromism and the different emission change upon fumed and annealed are explained by the later obtained single crystal data and the powder X-ray diffraction (PXRD) investigations of the unground (pristine), ground, and recovered samples.

To investigate the underlying origin of the mechanochromism of TDMAPE, two polymorphs of TDMAPE with different fluorescent emissions were obtained by slow evaporation of its n-hexane/dichloromethane solution (Figure 3a). The detailed cultivation process of the two single crystals can be seen in the Supporting Information. And the two crystals were named as TDMAPE-blue (Em = 460 nm) and TDMAPE-green (Em = 497 nm) according to their emission peaks, respectively (Figure 3b). In addition, both of the two crystals possess high quantum yield and long lifetime (TDMAPE-blue: 98%, 3.51 ns; TDMAPE-green: 67%, 3.69 ns). Their ORTEP drawings are shown in Figure S2, and the crystal data are given in Table S2.
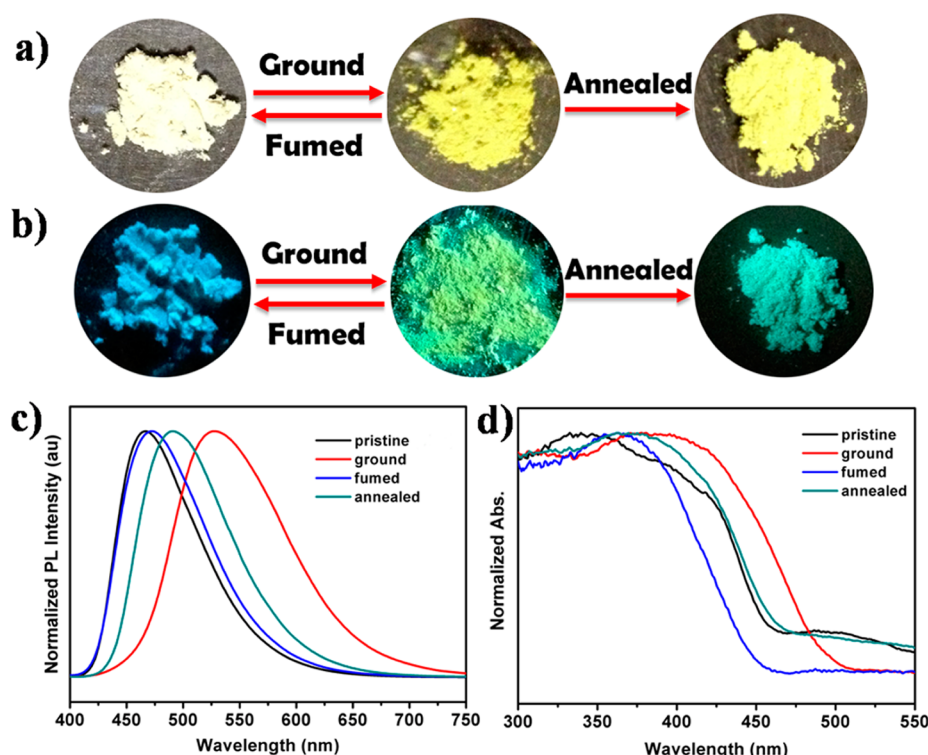
Figure 2. (a, b) Pictures of TDMAPE blue emission sample with different treatment taken under ambient light and UV irradiation (365 nm). (c, d) Corresponding fluorescence spectra and diffused reflectance absorption spectra.
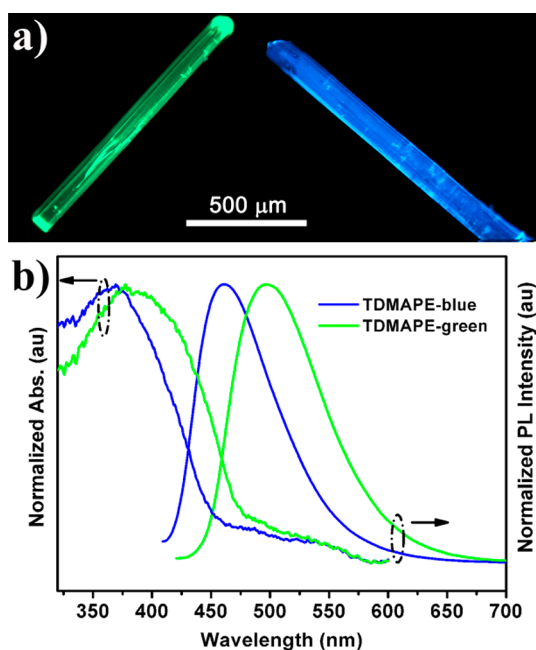

Figure 3. (a) Fluorescence pictures of two single crystals. (b) Corresponding absorption spectra and fluorescence spectra of two single crystals.

Both crystals belong to the monoclinic system, with the space group $P21/c$ for blue and $C2/c$ for green. The molecule in TDMAPE-blue crystal possesses an asymmetric conformation, while the one in TDMAPE-green crystal has a symmetric conformation (Figure S3). Owing to the twisted structure of TPE, the molecules in both crystals are separated from each other, and thus crystals are mainly constructed by the

intermolecular interactions between the peripheral moieties as summarized in Figure S4 and Table S3.[50,51] Such stacking modes prevent molecules from coming close to form intermolecular $\pi-\pi$ stacking which will have a significant effect on the emission,[52] because the excimer formed due to the $\pi-\pi$ stacking usually has a red-shifted emission comparing to the emission of monomer. On the other hand, the interactions between the transition dipoles of the adjacent molecules are weak due to the large intermolecular distance.[53] Thus, here we can infer that the red-shift of emission after grinding may be mainly dependent on the intramolecular conformation. Indeed, the dihedral angles between four peripheral benzene rings and the ethylene core of the two crystals are totally different, which indicates there may be some differences in coplanarity in the single molecule level (see in Table S4). In order to compare the difference in coplanarity and conjugation degree, bond length alternation (BLA), a critical parameter determining the bandgap and conjugation of π-delocalized systems, is used for the estimation of the conjugation difference in TDMAPE-blue and TDMAPE-green based on the exact molecular conformations in the crystals.[54] BLA is calculated to be 0.038 43 for TDMAPE-blue, and 0.038 30 for TDMAPE-green. The smaller BLA value for TDMAPE-green suggests the better molecular coplanarity and conjugation than TDMAPE-blue.[54,55] Additionally, dimethylamino groups are strong electron-donating groups, which significantly influence molecular coplanarity and the fluorescent emission. Thus, we measured the dihedral angles between peripheral benzene rings and the dimethylamino groups. As shown in Table S5, the average dihedral angles of TDMAPE-blue are obviously larger than those of TDMAPE-green, which directly shows that TDMAPE-green has better coplanarity and larger conjugation than TDMAPE-blue. Furthermore, theoretical calculation on the bandgaps of TDMAPE-blue and TDMAPE-green were performed using

Table 1. Summary of Photophysical Properties and Energy Gaps of Two Single Crystals[a]

crystal	λ_{em} (nm)	Φ_F (%)	τ (ns)	K_r (s^{-1})	K_{nr} (s^{-1})	BLA	ΔE (eV)
TDMAPE-blue	460	98	3.51	2.79×10^7	5.9×10^5	0.038 43	3.98
TDMAPE-green	497	67	3.69	1.82×10^7	8.94×10^6	0.038 30	3.84

[a]Abbreviations: λ_{em} = emission maximum, Φ_F = fluorescence quantum yield determined using a calibrated integrating sphere, τ = lifetime, ΔE = energy bandgap coming from theoretical DFT calculation, K_r = radiative transition rate constant, K_{nr} = nonradiative transition rate constant.
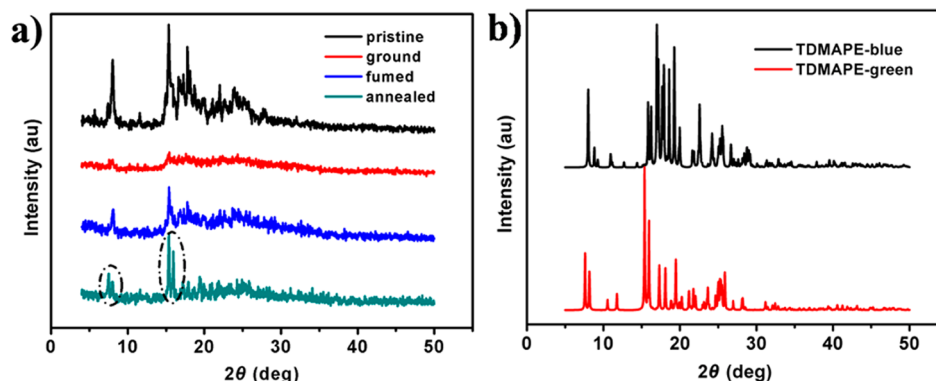

Figure 4. (a) PXRD patterns of TDMAPE blue emission sample: pristine, ground, fumed by ethyl acetate (EtOAc), and annealed (150 °C for 1 min). (b) Simulated PXRD patterns delineated on the basis of the crystal structure using the single crystal software Mercury 1.4.2.
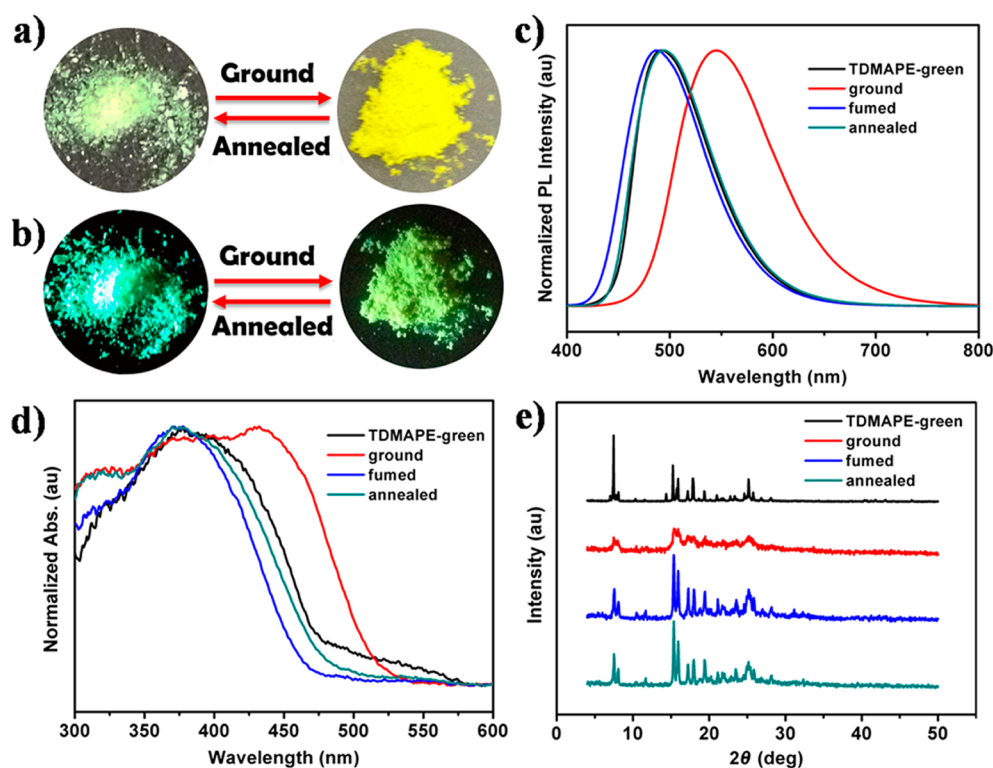

Figure 5. (a, b) Pictures of TDMAPE-green crystals with different treatment taken under ambient light and UV irradiation (365 nm). (c, d, e) Corresponding PL spectra, UV/vis reflection spectra, and PXRD patterns of TDMAPE-green crystals: pristine, ground, fumed by ethyl acetate (EtOAc), and annealed (150 °C for 1 min).

the B3LYP/6-31+g(d,p) basis set, and the results are given in Figure S5. The bandgap of TDMAPE-blue (3.98 eV) is calculated to be much larger than that of TDMAPE-green (3.84 eV), which is consistent with the absorption and emission spectra of the two crystals in Figure 3. All these evidence (summarized in Table 1) indicate that the increase of intramolecular coplanarity rather than the enhancement of π−π stacking can lead to the red-shift of emission. The result

further confirms that the proposed explanation for the red-shift of absorption and fluorescence spectra after grinding can be ascribed to the increased coplanarity and the decreased bandgap.

The PXRD measurements were carried on the sample to further investigate the mechanochromic properties of TDMAPE. And the PXRD patterns show that the mechano-chromism of TDMAPE is directly caused by crystalline to

amorphous phase transition. As can be seen in Figures 4a and 4b, the PXRD pattern of the pristine powder is accorded well with the simulated pattern from the single crystal data of TDMAPE-blue, suggesting that the pristine powder was mainly composed of the microcrystals of TDMAPE-blue. Upon grinding, the crystalline structure almost converts to amorphous phase as indicated from the decreased intensity of PXRD patterns. However, the ground sample is an unstable state, and it will rapidly crystallize if fumed by EtOAc or annealing treatment as can be seen the immediately increase of intensity of PXRD patterns. Interestingly, comparing with pristine and fumed sample, the PXRD pattern of annealed sample has a totally different PXRD pattern, which reveals that the annealed sample is a new crystalline phase. Furthermore, it is found that the recovered sample by annealing treatment has a similar PXRD pattern as the simulated pattern from of TDMAPE-green (Figure 4b), which means that the packing pattern of TDMAPE-green is a thermally stable state. Additionally, it was also supported by thermochromism of single crystal TDMAPE-blue as displayed thermally induced phase transformation to TDAMPE-green. When initial TDMAPE-blue was heated to 200 °C for 5 min, the green-emitting solid sample was formed (Figure S6). The emission wavelength of TDMAPE-blue was red-shifted about 26 nm from 460 to 486 nm by annealing treatment. In fact, this solid–solid phase transition (from TDMAPE-blue to TDAMPE-green) with obvious fluorescence change is associated with the first-order endothermic peak in the differential scanning calorimetry (DSC) thermogram (Figure S7). The broad endothermic peak around 150 °C refers to the crystal phase conversion, and the sharp endothermic peak at 328 °C corresponds to the melting point. Deserving to be mentioned, the fluorescent lifetime of the ground sample decreased from 3.35 to 2.69 ns. And comparing with the pristine blue emission powder, the ground sample has a decreased fluorescence quantum yield from 95% (before grinding) to 35% (after grinding). It can be ascribed to the increased nonradiative transition rate in Table S1. A more straightforward interpretation of the current result is that the existing intermolecular interactions in pristine powder have locked and rigidified the molecular conformation, largely reducing the energy loss via nonradiative relaxation channels.[17] Upon amphorization by mechanical force, some of these interactions are lost, which explains why the pristine microcrystals show stronger emission even though they possess a low conjugation.

In addition, it is worth mentioning that the TDMAPE-green crystals also have remarkable mechanochromic properties. As can be seen in Figure 5, the absorption and emission spectra also show an obvious red-shift after grinding and then will recover after fumed by EtOAc or annealing treatment. The PXRD pattern of TDMAPE-green crystals shows intense and sharp peaks agreeing well with the simulated peaks from the single crystal data (Figures 5e and 4b). In contrast, the ground sample of TDMAPE-green shows a small and broad diffraction intensity. The significant decrease of the signal intensity indicates that grinding can convert crystalline to amorphous phase. However, the amorphous phase is an unstable state, and it will recover to a stable state after recrystallization with solvent or heat, as evidenced by the immediately recovered intense and sharp reflections. Here, it did not show obvious difference of PXRD patterns between the two types of recover treatment. On the other hand, the fluorescence quantum yield of ground sample increased from 67% (TDMAPE-green) to 95% (after

grinding). Meanwhile, the fluorescent lifetime of ground sample increased remarkably from 3.69 ns (before grinding) to 4.10 ns (after grinding). The increased quantum yield and lifetime after grinding is directly resulting from the increased radiative transition rate and the decreased nonradiative transition rate (see Table S1). After carefully comparing the PXRD patterns of the ground samples of TDMAPE-blue and TDMAPE-green, we can find the diffraction peaks almost disappeared for TDMAPE-blue, but only weaken and broaden for TDMAPE-green. Considering the totally different weak interactions in two crystals, we infer the weaker C−H···π interaction in TDMAPE-blue is easier to be broken, while the C−H···N interaction in TDMAPE-green is much stronger as it did not show obvious lost after grinding. Therefore, the energy loss via nonradiative relaxation channels can be prevented for the ground sample of TDMAPE-green. On the other hand, the increased intra-molecular coplanarity after grinding seems to show its important role as the extended conjugation by grinding will indeed increase the radiative transition rate. In other words, the underlying reason for the slightly increased quantum yield may result from the increased conjugation of the ground sample. Like the mechanochromic explanation of the blue emission powder mentioned earlier, the above evidence indicated that the red-shift can be ascribed to the increased coplanarity.

In summary, TDMAPE, a simple molecule, was found to have mechanochromic property and polymorphism-dependent emission. The mechanochromism and polymorphism were investigated by absorption spectra, PXRD patterns, single crystal structures, and theoretical calculations, which indicate that the red-shift of the emission by grinding is mainly determined by the intramolecular conformation rather than π−π stacking and H- or J-aggregation. As the TDMAPE molecule has a twisted conformation, it seems that it will have increased coplanarity and larger conjugation after grinding, which decreased the optical bandgap and ultimately led to the bathochromic shift of the emission.

■ ASSOCIATED CONTENT

Ⓢ Supporting Information
Details of characterization and measurement; TEM images and ED patterns of aggregations of TDMAPE; crystal structure data for TDMAPE-green and TDMAPE-blue (CCDC 934490 and 934491) (CIF) and their structural diagrams; unit cell structures, intermolecular weak interactions, torsion angles, and theoretical calculation data of the two polymorphs. This material is available free of charge via the Internet at http://pubs.acs.org.

■ AUTHOR INFORMATION

Corresponding Authors
*E-mail wjtian@jlu.edu.cn (W.T.).
*E-mail xubin@jlu.edu.cn (B.X.).
Notes
The authors declare no competing financial interest.

■ ACKNOWLEDGMENTS

■ REFERENCES

(1) Sagara, Y.; Kato, T. Mechanically Induced Luminescence Changes in Molecular Assemblies. *Nat. Chem.* **2009**, *1*, 605−610.

(2) Sagara, Y.; Yamane, S.; Mutai, T.; Araki, K.; Kato, T. A Stimuli-Responsive, Photoluminescent, Anthracene-Based Liquid Crystal: Emission Color Determined by Thermal and Mechanical Processes. *Adv. Funct. Mater.* **2009**, *19*, 1869−1875.

(3) Kinami, M.; Crenshaw, B. R.; Weder, C. Polyesters with Built-in Threshold Temperature and Deformation Sensors. *Chem. Mater.* **2006**, *18*, 946−955.

(4) Pucci, A.; Cuia, F. D.; Signori, F.; Ruggeri, G. Bis(benzoxazolyl)-stilbene Excimers as Temperature and Deformation Sensors for Biodegradable Poly(1,4-butylene succinate) Films. *J. Mater. Chem.* **2007**, *17*, 783−790.

(5) Zhang, X.; Chi, Z.; Li, H.; Xu, B.; Li, X.; Zhou, W.; Liu, S.; Zhang, Y.; Xu, J. Piezofluorochromism of an Aggregation-Induced Emission Compound Derived from Tetraphenylethylene. *Chem.—Asian J.* **2011**, *6*, 808−811.

(6) Xu, B.; Chi, Z.; Zhang, J.; Zhang, X.; Li, H.; Li, X.; Liu, S.; Zhang, Y.; Xu, J. Piezofluorochromic and Aggregation-Induced-Emission Compounds Containing Triphenylethylene and Tetraphenylethylene Moieties. *Chem.—Asian J.* **2011**, *6*, 1470−1478.

(7) Li, H.; Zhang, X.; Chi, Z.; Xu, B.; Zhou, W.; Liu, S.; Zhang, Y.; Xu, J. New Thermally Stable Piezofluorochromic Aggregation-Induced Emission Compounds. *Org. Lett.* **2011**, *13*, 556−559.

(8) Li, H.; Chi, Z.; Xu, B.; Zhang, X.; Li, X.; Liu, S.; Zhang, Y.; Xu, J. Aggregation-Induced Emission Enhancement Compounds Containing Triphenylamine-Anthrylenevinylene and Tetraphenylethene Moieties. *J. Mater. Chem.* **2011**, *21*, 3760−3767.

(9) Xu, B.; Chi, Z.; Zhang, X.; Li, H.; Chen, C.; Liu, S.; Zhang, Y.; Xu, J. A New Ligand and Its Complex with Multi-Stimuli-Responsive and Aggregation-Induced Emission Effects. *Chem. Commun.* **2011**, *47*, 11080−11082.

(10) Zhang, X.; Chi, Z.; Xu, B.; Chen, C.; Zhou, X.; Zhang, Y.; Liu, S.; Xu, J. End-Group Effects of Piezofluorochromic Aggregation-Induced Enhanced Emission Compounds Containing Distyrylanthracene. *J. Mater. Chem.* **2012**, *22*, 18505−18513.

(11) Xu, B.; Xie, M.; He, J.; Xu, B.; Chi, Z.; Tian, W.; Jiang, L.; Zhao, F.; Liu, S.; Zhang, Y.; Xu, Z.; Xu, J. An Aggregation-Induced Emission Luminophore with Multi-Stimuli Single- and Two-Photon Fluorescence Switching and Large Two-Photon Absorption Cross Section. *Chem. Commun.* **2013**, *49*, 273−275.

(12) Zhou, X.; Li, H.; Chi, Z.; Zhang, X.; Zhang, J.; Xu, B.; Zhang, Y.; Liu, S.; Xu, J. Piezofluorochromism and Morphology of a New Aggregation-Induced Emission Compound Derived from Tetraphenyl-ethylene and Carbazole. *New J. Chem.* **2012**, *36*, 685−693.

(13) Luo, J.; Li, L. Y.; Song, Y.; Pei, J. A Piezochromic Luminescent Complex: Mechanical Force Induced Patterning with a High Contrast Ratio. *Chem.—Eur. J.* **2011**, *17*, 10515−10519.

(14) Chi, Z.; Zhang, X.; Xu, B.; Zhou, X.; Ma, C.; Zhang, Y.; Liu, S.; Xu, J. Recent Advances in Organic Mechanofluorochromic Materials. *Chem. Soc. Rev.* **2012**, *41*, 3878−3896.

(15) Zhao, N.; Yang, Z.; Lam, J. W. Y.; Sung, H. H. Y.; Xie, N.; Chen, S.; Su, H. M.; Gao, M.; Williams, I. D.; Wong, K. S.; Tang, B. Z. Benzothiazolium-Functionalized Tetraphenylethene: An AIE Lumi-nogen with Tunable Solid-State Emission. *Chem. Commun.* **2012**, *48*, 8637−8639.

(16) Chen, F.; Zhang, J.; Wan, X. Design and Synthesis of Piezochromic Materials Based on Push−Pull Chromophores: A Mechanistic Perspective. *Chem.—Eur. J.* **2012**, *18*, 4558−4567.

(17) Yuan, W. Z.; Tan, Y.; Gong, Y.; Lu, P.; Lam, J. W. Y.; Shen, X. Y.; Feng, C.; Sung, H. H. Y.; Lu, Y.; Williams, I. D.; Sun, J. Z.; Zhang, Y.; Tang, B. Z. Synergy between Twisted Conformation and Effective Intermolecular Interactions: Strategy for Efficient Mechanochromic Luminogens with High Contrast. *Adv. Mater.* **2013**, *25*, 2837−2843.

(18) Zhang, Z.; Yao, D.; Zhou, T.; Zhang, H.; Wang, Y. Reversible Piezo- and Photochromic Behaviors Accompanied by Emission Color Switching of Two Anthracene-Containing Organic Molecules. *Chem. Commun.* **2011**, *47*, 7782−7784.

(19) Mizoshita, N.; Tani, T.; Inagaki, S. Isothermally Reversible Fluorescence Switching of a Mechanochromic Perylene Bisimide Dye. *Adv. Mater.* **2012**, *24*, 3350−3355.

(20) Yoon, S. J.; Chung, J. W.; Gierschner, J.; Kim, S. K.; Choi, M. G.; Kim, D.; Park, S. Y. Multistimuli Two-Color Luminescence Switching via Different Slip-Stacking of Highly Fluorescent Molecular Sheets. *J. Am. Chem. Soc.* **2010**, *132*, 13675−13683.

(21) Dong, Y.; Xu, B.; Zhang, J.; Tian, X.; Wang, L.; Chen, J.; Lv, H.; Wen, S.; Li, B.; Ye, L.; Zou, B.; Tian, W. Piezochromic Luminescence Based on the Molecular Aggregation of 9,10-Bis((E)-2-(pyrid-2-yl)vinyl)anthracene. *Angew. Chem., Int. Ed.* **2012**, *51*, 10782−10785.

(22) Huang, J.; Yang, X.; Li, X.; Chen, P.; Tang, R.; Li, F.; Lu, P.; Ma, Y.; Wang, L.; Qin, J.; Li, Q.; Li, Z. Bipolar AIE-Active Luminogens Comprised of an Oxadiazole Core and Terminal TPE Moieties as a New Type of Host for Doped Electroluminescence. *Chem. Commun.* **2012**, *48*, 9586−9588.

(23) Huang, J.; Yang, X.; Wang, J.; Zhong, C.; Wang, L.; Qin, J.; Li, Z. New Tetraphenylethene-Based Effcient Blue Luminophors: Aggregation Induced Emission and Partially Controllable Emitting Color. *J. Mater. Chem.* **2012**, *22*, 2478−2484.

(24) Xu, X.; Huang, J.; Li, J.; Yan, J.; Qin, J.; Li, Z. A Graphene Oxide-Based AIE Biosensor with High Selectivity Toward Bovine Serum Albumin. *Chem. Commun.* **2011**, *47*, 12385−12387.

(25) Wang, M.; Zhang, G.; Zhang, D.; Zhu, D.; Tang, B. Z. Fluorescent Bio/Chemosensors Based on Silole and Tetraphenyle-thene Luminogens with Aggregation-Induced Emission Feature. *J. Mater. Chem.* **2010**, *20*, 1858−1867.

(26) Zhao, Z.; Chen, S.; Shen, X.; Mahtab, F.; Yu, Y.; Lu, P.; Lam, J. W. Y.; Kwok, H. S.; Tang, B. Z. Aggregation-Induced Emission, Self-Assembly, and Electroluminescence of 4,4′-Bis(1,2,2-triphenylvinyl)-biphenyl. *Chem. Commun.* **2010**, *46*, 686−688.

(27) Hong, Y.; Meng, L.; Chen, S.; Leung, C. W. T.; Da, L. T.; Faisal, M.; Silva, D. A.; Liu, J.; Lam, J. W. Y.; Huang, X.; Tang, B. Z. Monitoring and Inhibition of Insulin Fibrillation by a Small Organic Fluorogen with Aggregation-Induced Emission Characteristics. *J. Am. Chem. Soc.* **2012**, *134*, 1680−1689.

(28) Tong, H.; Hong, Y.; Dong, Y.; Häussler, M.; Li, Z.; Lam, J. W. Y.; Dong, Y.; Sung, H. H. Y.; Williams, I. D.; Tang, B. Z. Protein Detection and Quantitation by Tetraphenylethene-Based Fluorescent Probes with Aggregation-Induced Emission Characteristics. *J. Phys. Chem. B* **2007**, *111*, 11817−11823.

(29) Liu, Y.; Deng, C.; Tang, L.; Qin, A.; Hu, R.; Sun, J. Z.; Tang, B. Z. Specific Detection of d-Glucose by a Tetraphenylethene-Based Fluorescent Sensor. *J. Am. Chem. Soc.* **2011**, *133*, 660−663.

(30) Zhao, N.; Yang, Z.; Lam, J. W. Y.; Sung, H. H. Y.; Xie, N.; Chen, S.; Su, H.; Gao, M.; Williams, I. D.; Wong, K. S.; Tang, B. Z. Benzothiazolium-Functionalized Tetraphenylethene: an AIE Lumino-gen with Tunable Solid-State Emission. *Chem. Commun.* **2012**, *48*, 8637−8639.

(31) Wang, J.; Mei, J.; Hu, R.; Sun, J. Z.; Qin, A.; Tang, B. Z. Click Synthesis, Aggregation-Induced Emission, E/Z Isomerization, Self-Organization, and Multiple Chromisms of Pure Stereoisomers of a Tetraphenylethene-Cored Luminogen. *J. Am. Chem. Soc.* **2012**, *134*, 9956−9966.

(32) Luo, X.; Zhao, W.; Shi, J.; Li, C.; Liu, Z.; Bo, Z.; Dong, Y. Q.; Tang, B. Z. Reversible Switching Emissions of Tetraphenylethene Derivatives among Multiple Colors with Solvent Vapor, Mechanical, and Thermal Stimuli. *J. Phys. Chem. C* **2012**, *116*, 21967−21972.

(33) Li, C.; Luo, X.; Zhao, W.; Li, C.; Liu, Z.; Bo, Z.; Dong, Y.; Dong, Y. Q.; Tang, B. Z. Switching the Emission of Tetrakis(4-methoxyphenyl)ethylene Among Three Colors in the Solid State. *New J. Chem.* **2013**, *37*, 1696−1699.

(34) Luo, X.; Li, J.; Li, C.; Heng, L.; Dong, Y. Q.; Liu, Z.; Bo, Z.; Tang, B. Z. Reversible Switching of the Emission of Diphenyldi-benzofulvenes by Thermal and Mechanical Stimuli. *Adv. Mater.* **2011**, *23*, 3261−3265.

(35) Gu, X.; Yao, J.; Zhang, G.; Yan, Y.; Zhang, C.; Peng, Q.; Liao, Q.; Wu, Y.; Xu, Z.; Zhao, Y.; Fu, H.; Zhang, D. Polymorphism-Dependent Emission for Di(p-methoxylphenyl)dibenzofulvene and

25002

dx.doi.org/10.1021/jp407965a | *J. Phys. Chem. C* 2013, 117, 24997−25003

Analogues: Optical Waveguide/Amplified Spontaneous Emission Behaviors. *Adv. Funct. Mater.* **2012**, *22*, 4862−4872.

(36) Yoon, S. J.; Park, S. Y. Polymorphic and Mechanochromic Luminescence Modulation in the Highly Emissive Dicyanodistyrylbenzene Crystal: Secondary Bonding Interaction in Molecular Stacking Assembly. *J. Mater. Chem.* **2011**, *21*, 8338−8346.

(37) Zhang, G.; Lu, J.; Sabat, M.; Fraser, C. L. Polymorphism and Reversible Mechanochromic Luminescence for Solid-State Difluoroboron Avobenzone. *J. Am. Chem. Soc.* **2010**, *132*, 2160−2162.

(38) Qi, Q.; Liu, Y.; Fang, X.; Zhang, Y.; Chen, P.; Wang, Y.; Yang, B.; Xu, B.; Tian, W.; Zhang, S. X. AIE (AIEE) and Mechanofluorochromic Performances of TPE-methoxylates: Effects of Single Molecular Conformations. *RSC Adv.* **2013**, *3*, 7996−8002.

(39) Duan, X. F.; Zeng, J.; Lü, J. W.; Zhang, Z. B. Insights into the General and Efficient Cross McMurry Reactions between Ketones. *J. Org. Chem.* **2006**, *71*, 9873−9876.

(40) Barr, J. W.; Bell, T. W.; Catalano, V. J.; Cline, J. I.; Phillips, D. J.; Procupez, R. Syntheses, Structures, and Photoisomerization of (E)- and (Z)-2-Tert-Butyl-9-(2,2,2-Triphenylethylidene)fluorene. *J. Phys. Chem. A* **2005**, *109*, 11650−11654.

(41) Cariati, E.; Lanzeni, V.; Tordin, E.; Ugo, R.; Botta, C.; Schieroni, A. G.; Sironi, A.; Pasini, D. Efficient Crystallization Induced Emissive Materials Based on a Simple Push-Pull Molecular Structure. *Phys. Chem. Chem. Phys.* **2011**, *13*, 18005−18014.

(42) Coluccini, C.; Sharma, A. K.; Merli, D.; Griend, D. V.; Mannucci, B.; Pasini, D. Spectroscopic and Electrochemical Sensing of Lanthanides with π-Extended Chromophores Incorporating Ferrocenes and a Coordinative End. *Dalton Trans.* **2011**, *40*, 11719−11725.

(43) Coluccini, C.; Sharma, A. K.; Caricato, M.; Sironi, A.; Cariati, E.; Righetto, S.; Tordin, E.; Botta, C.; Forni, A.; Pasini, D. Switching of Emissive and NLO Properties in Push-Pull Chromophores with Crescent PPV-Like Structures. *Phys. Chem. Chem. Phys.* **2013**, *15*, 1666−1674.

(44) Luo, J.; Xie, Z.; Lam, J. W. Y.; Cheng, L.; Chen, H.; Qiu, C.; Kwok, H. S.; Zhan, X.; Liu, Y.; Zhu, D.; Tang, B. Z. Aggregation-Induced Emission of 1-Methyl-1,2,3,4,5-Pentaphenylsilole. *Chem. Commun.* **2001**, 1740−1741.

(45) Chen, J.; Law, C. C. W.; Lam, J. W. Y.; Dong, Y.; Lo, S. M. F.; Williams, I. D.; Zhu, D.; Tang, B. Z. Synthesis, Light Emission, Nanoaggregation, and Restricted Intramolecular Rotation of 1,1-Substituted 2,3,4,5-Tetraphenylsiloles. *Chem. Mater.* **2003**, *15*, 1535−1546.

(46) Chen, J.; Xu, B.; Ouyang, X.; Tang, B. Z.; Cao, Y. Aggregation-Induced Emission of cis,cis-1,2,3,4-Tetraphenylbutadiene from Restricted Intramolecular Rotation. *J. Phys. Chem. A* **2004**, *108*, 7522−7526.

(47) Ren, Y.; Lam, J. W. Y.; Dong, Y.; Tang, B. Z.; Wong, K. S. Enhanced Emission Efficiency and Excited State Lifetime Due to Restricted Intramolecular Motion in Silole Aggregates. *J. Phys. Chem. B* **2005**, *109*, 1135−1140.

(48) Hong, Y.; Lam, J. W. Y.; Tang, B. Z. Aggregation-Induced Emission: Phenomenon, Mechanism and Applications. *Chem. Commun.* **2009**, *29*, 4332−4353.

(49) Hong, Y.; Lam, J. W. Y.; Tang, B. Z. Aggregation-Induced Emission. *Chem. Soc. Rev.* **2011**, *40*, 5361−5388.

(50) Tsuzuki, S. CH/π Interactions. *Annu. Rep. Prog. Chem., Sect. C: Phys. Chem.* **2012**, *108*, 69−95.

(51) Taylor, R.; Kennard, O. Crystallographic Evidence for the Existence of C-H⋯O, C-H⋯N, and C-H⋯Cl Hydrogen Bonds. *J. Am. Chem. Soc.* **1982**, *104*, 5063−5070.

(52) Hunter, C. A.; Sanders, J. K. M. The Nature of π-π Interactions. *J. Am. Chem. Soc.* **1990**, *112*, 5525−5534.

(53) Kasha, M.; Rawls, H. R.; El-Bayoumi, M. A. The Excition Model in Molecular Spectroscopy. *Pure Appl. Chem.* **1965**, *11*, 371−392.

(54) Ohira, S.; Hales, J. M.; Thorley, K. J.; Anderson, H. L.; Perry, J. W.; Brédas, J. L. A New Class of Cyanine-like Dyes with Large Bond-Length Alternation. *J. Am. Chem. Soc.* **2009**, *131*, 6099−6101.

(55) Yang, S.; Kertesz, M. Bond Length Alternation and Energy Band Gap of Polyyne. *J. Phys. Chem. A* **2006**, *110*, 9771−9774.